ChemComm

COMMUNICATION

View Article Online
View Journal | View Issue

Cite this: *Chem. Commun.*, 2022, **58**, 9369

Received 27th June 2022,
Accepted 27th July 2022

DOI: 10.1039/d2cc03574j

rsc.li/chemcomm

Highly selective molecular sieving of *cis*- over *trans*-1,2-dichloroethene isomers†

Xin Liu, Lukman O. Alimi and Niveen M. Khashab *

An intrinsically porous trianglimine macrocycle 1 is reported to display energy-efficient and cost-effective adsorptive properties by selectively separating *cis*-1,2-dichloroethene (*cis*-DCE) from an equimolar *cis*- and *trans*-DCE mixture with a purity of over 96%. The selectivity is enhanced by host/guest C–H···π intermolecular interactions. Moreover, the macrocycle can be reused many times without any decrease in performance, which further supports the sustainability of using molecular sieves in chemical separation.

Olefins are high-value raw materials in the chemical and petrochemical industries.[1,2] The separation of pure olefin derivatives using conventional technology is energy-intensive and time-consuming.[3,4] Haloalkenes are typical olefin derivatives, which are mainly produced by direct halogenation of alkenes and obtained as a mixture (*cis*–*trans* isomers).[5,6] Each isomer has a specific application in the polymer industry and synthetic field.[7–9] For instance, *trans*-1,2-dichloroethene (*trans*-DCE) is used in the extraction of rubber and as a refrigerant, while *cis*-1,2-dichloroethene (*cis*-DCE) is a foam-blowing additive.[10,11] Thus, obtaining the pure *cis*- and *trans*-DCE isomers is of great industrial and economic importance. However, owing to the proximity of their molecular sizes and boiling points, it is still very challenging to employ fractional distillation with very high towers to separate the isomers with high purity.[12,13] Adsorptive separation using porous materials, such as metal organic frameworks, offers an economic and energy-efficient solution but nonthermally-driven adsorptive separation for *cis*–*trans* alkene isomers is still relatively unexplored.[14–23] Consequently, new adsorbents with good stability and economic feasibility are imperative and desirable towards the practical industrial separation of *cis*–*trans* isomers.[24]

Trianglimine macrocycles are a class of intrinsically porous materials that can be easily prepared and scaled up for selective separations.[25–28] In this work, we describe a trianglimine macrocycle **1** that can be used as a molecular sieve for efficient and successful separation of *cis*-DCE from an equimolar *cis*/*trans*-DCE mixture in both liquid and vapor phases (Scheme 1). The naphthalene sidewall increases the rigidity of the macrocycle and guest binding ability.[29,30] Meanwhile, the removal of the trapped guests could transform the macrocycle **1** crystals back to the original guest-free form, endowing the macrocycle with excellent recyclability and reversibility (Fig. 1).

Macrocycle **1** was successfully prepared by an imine condensation reaction (Scheme S1, ESI†), as verified by detailed characterizations (Fig. S1–S3, ESI†). SCXRD analysis of macrocycle **1** in dichloromethane (DCM) (**1A**) showed a rigid intrinsic cavity of *ca.* 4.0 Å and demonstrated that macrocycle **1A** crystallises in a monoclinic system with a $P2_1$ space group and the asymmetric unit contains one unit each of the macrocycle and DCM (Fig. S4 and Table S1, ESI†). The structure analysis also indicated that the macrocycle **1A** is packed in a head–tail fashion along the *b* axis where the DCM occupied the channels (Fig. S5, ESI†). The activated macrocycle (**1α**) was obtained after activation of **1A** at 80 °C for 24 h under a high vacuum. Thermogravimetric analysis (TGA) showed that macrocycle **1A** loses DCM to obtain the guest-free material **1α** that was used for further adsorption experiments (Fig. S6, ESI†). PXRD analysis revealed that **1α** retains its crystallinity even after the removal of solvent molecules from the channels (Fig. 1 and Fig. S7, ESI†).

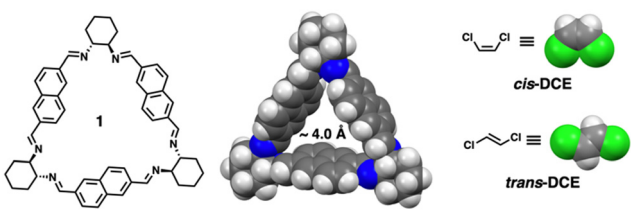

Scheme 1 Chemical structure of macrocycle **1**, *cis*- and *trans*-DCE.

Smart Hybrid Materials Laboratory (SHMs), Advanced Membranes and Porous Materials Center, King Abdullah University of Science and Technology (KAUST), Thuwal 23955-6900, Kingdom of Saudi Arabia.
E-mail: niveen.khashab@kaust.edu.sa

† Electronic supplementary information (ESI) available. CCDC 2177715–2177718. For ESI and crystallographic data in CIF or other electronic format see DOI: https://doi.org/10.1039/d2cc03574j

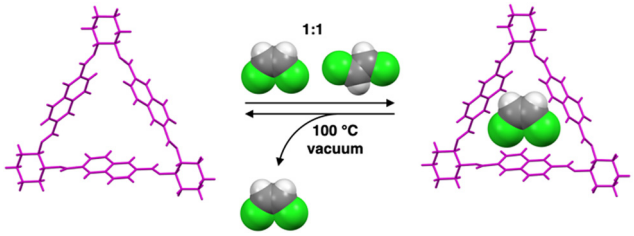

Fig. 1 Crystal structure of macrocycle **1** showing the selectivity of *cis*-DCE over *trans* in a *cis*/*trans*-DCE mixture.

The macrocycle **1α** did not adsorb N_2 at 77 K and CO_2 at 298 K, indicating a nonporous material (Fig. S8, ESI†). However, previous reports based on trianglimine with approximate porosity showed significant molecular recognition features.[26,28]

To investigate the porosity and selectivity of crystalline **1α** towards *cis*/*trans*-DCE isomers, single component and equimolar isomer mixture solid–vapor adsorption experiments were conducted at 298 K for commercially pure *cis*- and *trans*-DCE. The ^{1}H NMR result revealed the significant uptake of *cis*-DCE and the negligible uptake of *trans*-DCE and confirmed the selective adsorption of *cis*-DCE over *trans*-DCE from the mixture with a high selectivity of over 92% (Fig. S9–S11, ESI†). PXRD experiments were performed to further support the preference of **1α** towards *cis*-DCE over *trans*-DCE. PXRD patterns of **1α** displayed structural transformation upon exposure to *cis*-DCE, indicating the adsorption of *cis*-DCE. However, the PXRD patterns of **1α** showed negligible change after being exposed to *trans*-DCE. Moreover, **1α** after exposure to an equimolar mixture of *cis*/*trans*-DCE vapors showed preferred adsorption of *cis*-DCE over *trans*-DCE (Fig. 2).

To better understand the host–guest interactions in the guest-induced adsorption process, single crystals of **1** with *cis*-DCE and *trans*-DCE were grown by vapor diffusion of methanol into a *cis*- or *trans*-DCE solution.[26,31] A 1 : 1 host–guest complex formed for *cis*-DCE loaded **1** (*cis*-DCE@**1**, Fig. 3a). SCXRD analysis indicated that the complex crystallises in a monoclinic crystal system with $P2_1$ space group and the asymmetric unit contains one unit of each macrocycle and *cis*-DCE (Fig. S12 and Table S1, ESI†). The space-filling model revealed that *cis*-DCE best fits in the intrinsic cavity of **1** (Fig. 3a). Each *cis*-DCE entrapped in the intrinsic cavity of **1** is stabilized by host–guest C–H···π interaction (Fig. 3b and Table S2, ESI†). The macrocycle units are connected to one another by C–H···π and C–H···N interactions to form a layered structure (Fig. S12e and Table S3, ESI†). The window to window packing mode of macrocycle molecules contributes to the formation of channels that can trap *cis*-DCE in the internal cavity of the aligned macrocycles along *b* axis (Fig. 3c). Thermogravimetric analysis (TGA) showed a weight loss of 9.1% up to 100 °C, indicating a 1 : 1 host–guest ratio of **1** and *cis*-DCE (Fig. S13, ESI†). However, the single crystal of **1** grown in *trans*-DCE showed only the macrocycle crystals without the *trans*-DCE guest molecule in its cavity (Fig. S14, ESI†). This reveals that macrocycle **1** is selective towards the *cis*-DCE isomer. Furthermore, PXRD patterns of *cis*- and *trans*-DCE with **1** match well with the simulated pattern (Fig. S15a and b, ESI†).

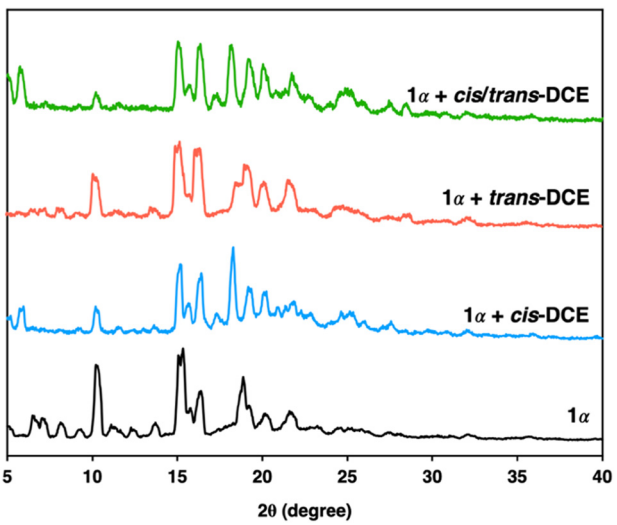

Fig. 2 Experimental PXRD patterns of **1α** before and after exposure to *cis*- or *trans*-DCE for 1 h.

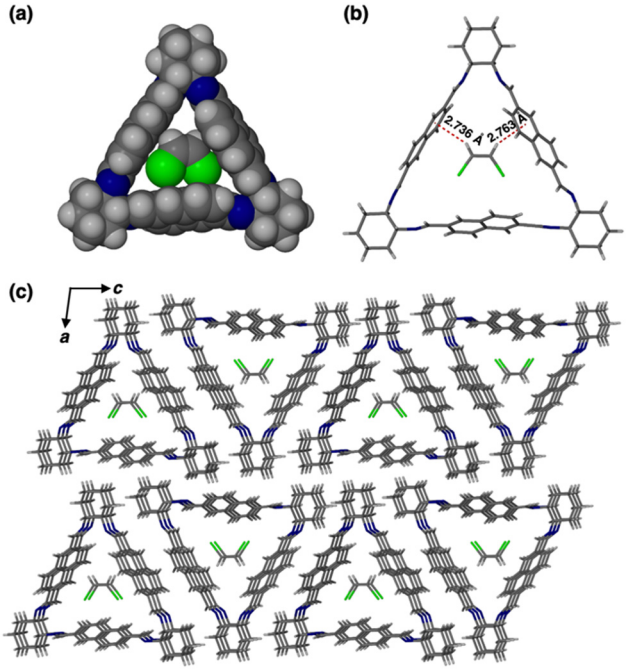

Fig. 3 Single crystal structure of *cis*-DCE@**1**. (a) Space filling model shows that *cis*-DCE fits the intrinsic pore of the host. (b) Illustration of the C–H···π interaction between *cis*-DCE and macrocycle **1**. (c) Packing arrangements of single crystal.

This observation prompted us to investigate the competitive crystallisation of **1** with a 1 : 1 v/v mixture of *cis*- and *trans*-DCE. The obtained crystals revealed an exact structure of *cis*-DCE@**1** (Fig. S16 and Table S1, ESI†). GC analysis further confirmed that *cis*-DCE isomer was selectively absorbed and separated with a high purity of over 99% (Fig. S17, ESI†). PXRD patterns and TGA of competitive experiments were further tested for an

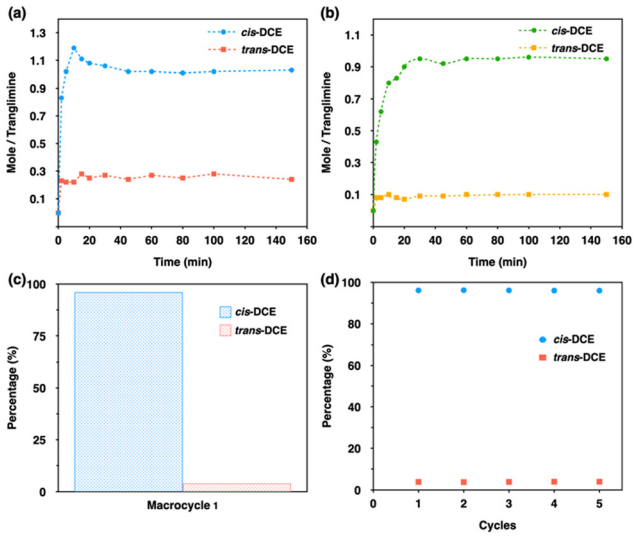

Fig. 4 (a) Time-dependent solid–vapor sorption plot of **1α** for single-component *cis*- and *trans*-DCE. (b) Time-dependent solid–vapor sorption plot of **1α** in *cis*/*trans*-DCE (1 : 1 v/v) mixture. (c) Relative uptake of *cis*- and *trans*-DCE over 1 h. (d) Relative uptake capacity of crystalline **1A** towards *cis*/*trans*-DCE (1 : 1 v/v) mixture for 5 cycles.

equimolar mixture of *cis*- and *trans*-DCE, which also supported the selectivity towards *cis* isomer (Fig. S15c and S18, ESI†). It was found that the internal cavity was stabilized by *cis*-DCE *via* C–H···π interaction in the crystal structure, while *trans*-DCE is unable to penetrate the cavity due to the size and shape mismatch that was also reflected in the selectivity (Fig. S16, ESI†). In addition to testing the selectivity with equimolar mixtures, we also performed different fractions of *cis*/*trans*-DCE mixtures and found that the selectivity toward *cis*-DCE still can be detected even with 2 : 8 mixtures (Fig. S19, ESI†).

To measure the detailed pathway and uptake rate for the selectivity of *cis* isomer, time-dependent solid–vapor adsorption studies were performed for single-component and equimolar mixtures. The uptake capacity for single-component increases very fast and reaches saturation within 40 min with *ca.* 1.0 *cis*-DCE molecule by one trianglimine. However, it was found that the uptake of *trans* isomer reaches saturation within 20 min with *ca.* 0.3 molecule by one macrocycle (Fig. 4a). Then we studied the time-dependent solid–vapor experiment for an equimolar mixture of *cis*- and *trans*-DCE using **1α**. The result revealed that the uptake of *cis*-DCE in **1α** increased over time and reached saturation within 40 min, while the adsorption of *trans* isomer was almost negligible throughout the entire period (Fig. 4b). The *cis* isomer uptake amount was one molecule per macrocycle. GC analysis confirmed the high selectivity towards *cis* isomer with a purity of 96.6% (Fig. 4c and Fig. S20, ESI†).

As we established that **1α** shows high selectivity towards *cis*-DCE over *trans*-DCE in both liquid and vapor phases (Fig. S21, ESI†), it is necessary to make it practically useful. In the industrial separation process, an adsorbent must be recyclable with reproducible applicability. In this case, recyclability and stability of crystalline **1A** were confirmed accordingly by GC and PXRD over five cycles with no significant loss in selectivity or performance (Fig. 4d and Fig. S22, ESI†).

Finally, we investigated the stability of the macrocycle **1** under possible harsh industrial conditions such as a highly basic, acidic and humid environment using ^{1}H NMR. ^{1}H NMR spectrum confirms that the macrocycle **1** remains stable after being kept in 1 M NaOH aqueous solution for five days. However, the incubation of macrocycle **1** in acidic conditions degrades the macrocycle. Moreover, the stability of the macrocycle **1** was also tested in an aqueous solution where it shows no sign of decomposition or dissolution after several days (Fig. S23 and S24, ESI†).

We have successfully demonstrated the selective properties of an intrinsically porous macrocycle **1** toward *cis*-and *trans*-DCE in solution and vapor phases with a high selectivity of over 96% for multiple cycles. Crystal structure analysis shows that the naphthalene side wall plays an important role due to the high rigidity of the macrocycle and increasing guest binding affinity by C–H···π interaction. The ease of fabrication, high separation efficiency, and good stability make macrocycle **1** a promising candidate for molecular sieves-based separation of isomers under mild conditions in the future.

Conflicts of interest

There are no conflicts to declare.

Notes and references

1 D. J. Safarik and R. B. Eldridge, *Ind. Eng. Chem. Res.*, 1998, **37**, 2571–2581.
2 A. H. Tullo, *Chem. Eng. News*, 2000, **78**, 21–31.
3 E.-L. Dreher, K. K. Beutel, J. D. Myers, T. Lubbe, S. Krieger and L. H. Pottenger, *Ullmann's Encyclopedia of Industrical Chemistry*, Wiley, 2014.
4 R. B. Eldridge, *Ind. Eng. Chem. Res.*, 1993, **32**, 2208–2212.
5 Y. Zhou, K. Jie, R. Zhao and F. Huang, *J. Am. Chem. Soc.*, 2019, **141**, 11847–11851.
6 J.-R. Wu, B. Li and Y.-W. Yang, *Angew. Chem., Int. Ed.*, 2020, **59**, 2251–2255.
7 X. Fang, L. Liu, J. Lei, D. He, S. Zhang, J. Zhou, F. Wang, H. Wu and H. Wang, *Nat. Mach. Intell.*, 2022, **4**, 127–134.
8 H. Futamata, N. Yoshida, T. Kurogi, S. Kaiya and A. Hirashi, *ISME J.*, 2007, **1**, 471–479.
9 Y. Nakayama, A. Ishikawa, R. Sato, K. Uchida and N. Kambe, *Polym. J.*, 2008, **40**, 1060–1066.
10 Encyclopedia of Toxicology, Philip Wexler, ISBN 9780123864550.
11 Y. Wang, K. Xu, B. Li, L. Cui, J. Li, X. Jia, H. Zhao, J. Fang and C. Li, *Angew. Chem., Int. Ed.*, 2019, **58**, 10281–10284.
12 K. A. Marshall, Chlorocarbons and Chlorohydrocarbons, Survey, *Kirk-Othmer Encyclopedia of Chemical Technology*, Wiley-Interscience, New York, 2003.
13 A. E. Wentink, D. Kockmann, N. J. M. Kuipers, A. B. de Haan, J. Scholtz and H. Mulder, *Sep. Purif. Technol.*, 2005, **43**, 149–162.
14 A. Cadiau, K. Adil, P. M. Bhatt, Y. Belmabkhout and M. Eddaoudi, *Science*, 2016, **353**, 137–140.
15 Y. Wu and B. M. Weckhuysen, *Angew. Chem., Int. Ed.*, 2021, **60**, 18930–18949.
16 H. Liu, Y. He, J. Jiao, D. Bai, D. Chen, R. Krishna and B. Chen, *Chem. – Eur. J.*, 2016, **22**, 14988–14997.
17 M. Maes, L. Alaerts, F. Vermoortele, R. Ameloot, S. Couck, V. Finsy, J. F. M. Denayer and D. E. De Vos, *J. Am. Chem. Soc.*, 2010, **132**, 2284–2292.

18 K. Jie, Y. Zhou, E. Li, R. Zhao, M. Liu and F. Huang, *J. Am. Chem. Soc.*, 2018, **140**, 3190–3193.
19 G. Zhang, B. Hua, A. Dey, M. Ghosh, B. A. Moosa and N. M. Khashab, *Acc. Chem. Res.*, 2021, **54**, 155–168.
20 J. Pei, K. Shao, L. Zhang, H.-M. Wen, B. Li and G. Dong, *Top. Curr. Chem.*, 2019, **377**, 33.
21 P.-Q. Liao, N.-Y. Huang, W.-X. Zhang, J.-P. Zhang and X.-M. Chen, *Science*, 2017, **356**, 1193–1196.
22 Z. Zhang, X. Cui, X. Jiang, Q. Ding, J. Cui, Y. Zhang, Y. Belmabkhout, K. Adil, M. Eddaoudi and H. Xing, *Engineering*, 2021, **11**, 80–86.
23 Z. Zhang, Q. Yang, X. Cui, L. Yang, Z. Bao, Q. Ren and H. Xing, *Angew. Chem., Int. Ed.*, 2017, **56**, 16282–16287.
24 B. Moosa, L. O. Alimi, A. Shkurenko, A. Fakim, P. M. Bhatt, G. Zhang, M. Eddaoudi and N. M. Khashab, *Angew. Chem., Int. Ed.*, 2020, **59**, 21367–21371.
25 A. Chaix, G. Mouchaham, A. Shkurenko, P. Hoang, B. Moosa, P. M. Bhatt, K. Adil, K. N. Salama, M. Eddaoudi and N. M. Khashab, *J. Am. Chem. Soc.*, 2018, **140**, 12571–12575.
26 Y. Ding, A. Dey, L. O. Alimi, P. M. Bhatt, J. Du, C. Maaliki, M. Eddaoudi, J. Jacquemin and N. M. Khashab, *Chem. Mater.*, 2022, **34**, 197–202.
27 A. Dey, S. Chand, B. Maity, P. M. Bhatt, M. Ghosh, L. Cavallo, M. Eddaoudi and N. M. Khashab, *J. Am. Chem. Soc.*, 2021, **143**, 4090–4094.
28 B. Hua, Y. Ding, L. O. Alimi, B. Moosa, G. Zhang, W. S. Baslyman, J. Sessler and N. M. Khashab, *Chem. Sci.*, 2021, **12**, 12286–12291.
29 X. Wang, F. Jia, L.-P. Yang, H. Zhou and W. Jiang, *Chem. Soc. Rev.*, 2020, **49**, 4176–4188.
30 X. Huang, X. Wang, M. Quan, H. Yao, H. Ke and W. Jiang, *Angew. Chem., Int. Ed.*, 2021, **60**, 1929–1935.
31 J. Cao, Y. Wu, Q. Li, W. Zhu, Z. Wang, Y. Liu, K. Jie, H. Zhu and F. Huang, *Chem. Sci.*, 2022, **13**, 7536–7540.

